

Gold Nanoparticle-Based Detection of Hg(II) in an Aqueous Solution: Fluorescence Quenching and Surface-Enhanced Raman Scattering Study

Erdene-Ochir Ganbold, Jin-Ho Park, Kwang-Su Ock, and Sang-Woo Joo*

Department of Chemistry, Soongsil University, Seoul 156-743, Korea. *E-mail: sjoo@ssu.ac.kr

Received September 8, 2010, Accepted December 3, 2010

We studied the detection of the Hg(II) concentration in an aqueous solution using rhodamine dyes on citrate-reduced Au nanoparticles (NPs). The quenching effect from Au NPs was found to decrease as the Hg(II) concentration increased under our experimental conditions. As the fluorescence signals intensified, the surface-enhanced Raman scattering (SERS) intensities reduced on the contrary due to less rhodamine dyes on Au NPs as the Hg(II) concentration increased. The rhodamine 6G (Rh6G) and rhodamine 123 (Rh123) dyes were examined via fluorescence and SERS measurements depending on Hg(II) concentrations. Fast and easy fluorescence detection of an Hg(II) concentration as low as a few ppm could be achieved by naked eye using citrate-reduced Au NPs.

Key Words: Gold nanoparticles, Mercury detection, Fluorescence quenching, Rhodamine dyes, SERS

Introduction

Because mercury(II) is one of the most toxic metal ions and damages various human organs,¹⁻² resulting in serious symptoms and health deterioration, its detection is necessary to protect people and the environment.³ Many currently employed spectroscopic techniques such as atomic absorption/emission, cold vapor atomic fluorescence spectrometry, or inductively coupled plasma mass spectrometry in use, require expensive and sophisticated instrumentation along with complicated sample preparation procedures.⁴

Fluorescent chemosensors have been widely tested for the detection of specific metal ions⁵ including Hg(II) ions due to their high sensitivity and selectivity.⁶ On the other hand, nanoparticles (NPs) may exhibit superior optical properties including photoluminescence.⁷ Among many NPs, gold (Au) have been currently used in the colorimetric detection of biological and environmental sensors.⁸ Fluorescence from organic dyes should be decreased in the presence of gold (Au) NPs because of their role as unique quenchers for chromophores through energy or electron transfer processes. This fluorescence was however found to increase as the Hg(II) concentration as a result of the binding of mercury ions and organic dyes. Although nanostructure-based fluorescence sensors for Hg(II) in an aqueous solution have been reported by several scientists,⁹ it has not been reported in detail yet regarding how the organic dyes should interact with Au NPs by means of either fluorescence measurements or vibrational analysis.

The surface enhanced Raman scattering (SERS) phenomenon has become one of the most sensitive techniques for monitoring the adsorbates on metallic substrates at the submonolayer coverage limit.¹⁰⁻¹⁴ SERS can detect a trace amount of organic contaminants in aqueous solutions with a sensitivity approaching single molecular identification. SERS has the advantage of clarifying chemical identity, biomolecules, and environmental pollutants adsorbed on metallic surfaces. Analysis of spectral features has provided detailed information on interfacial structures, adsorption mechanisms, and surface reactions. Few reports have

explored Hg ions' chemisorption onto metallic surfaces directly using SERS.¹⁵ Although there has been a recent fluorescence study,¹⁶ either a minute investigation of rhodamine dyes' chemisorption on Au NPs or a combined fluorescence measurements and SERS probing as a Hg(II) sensor has not been fully clarified to the best of our knowledge. In this work, we report on a spectroscopic study of Hg(II) detection of Rh6G and Rh123 using Au NP-based fluorescence and SERS for a better understanding of the adsorption of rhodamine dyes on Au NP surfaces in the presence of Hg ions.

Experimental Section

Rh6G, Rh123, HAuCl₄ and Mercury(II) chloride were purchased from Sigma-Aldrich. Rhodamine dyes (5×10^{-6} mol L⁻¹) were diluted with a solution of Au NPs by 10:1 respectively. 5×10^{-3} M sodium tetraborate at pH 9.0 was used to maintain the pH condition. A stock solution of Hg(II) was prepared by dissolving 11.1 mg of HgCl₂ in 10 mL distilled water containing a few drops of HCl, and was diluted further to make lower concentrations. Stock Hg(II) solution was diluted again down to 100 ppm. Stock solutions of rhodamine (5.0×10^{-6} mol L⁻¹) dyes were prepared in distilled water.

Approximately 10 mL aqueous solution containing 3 mL of HAuCl₄ (14 mM) was boiled in a vial with a magnetic stirring bar on a heating and stirring plate.¹⁷ A volume of 3 mL of sodium citrate (55 mM) was added to the above solution when it began to boil. A few minutes later the solution's color changed from yellow to deep red. The solution boiled for 1 hour while being stirring, and we added distilled water to maintain its volume. The maximum absorption is at ~520 nm. The morphologies of particles show that the particle shape is nearly spherical for the particles with a Tecnai F20 Philips transmission electron microscope after placing a drop of colloidal solution on a carbon-coated copper grid. The Au NPs' average size was ~20 nm. The particle's mean diameters and their relative standard deviations were obtained for each sample by counting at least 100 particles. We found the quenching effects for rhodamine dyes to be diff-

erent depending on the Au percentages in the aqueous solution. Due to their different molecular structures, the optimum concentrations of Au NPs inducing fluorescence quenching and SERS should be different for the tested rhodamine dyes. The initial Au percentages in NP solutions were better quantified to be ~140 ppm using a Perkin-Elmer OPTIMA 4300DV inductively coupled plasma-atomic emission spectrometer (ICP-AES). For the given synthesized Au NP solution, our data appeared to be consistent enough to discuss the reproducibility in a quantitative fashion.

Raman spectra were obtained using a Renishaw Raman confocal system model 1000 spectrometer equipped with an integral microscope (Leica DM LM).¹¹ Since our excitation wavelength at 633 nm was somewhat off from the absorption bands of the three rhodamine dyes, the Raman intensities from the detached dyes due to the resonance effects were not expected to quite significant. In the presence of Au NPs, the fluorescence signal decrease due to the quenching effect. The reproducibility is also examined by obtaining and averaging the data of SERS spectral intensities for rhodamine dyes on Au NPs by taking the samples repeatedly. Since we performed the SERS measurements in a rather homogenous aqueous solution, we did attempt to obtain the spectra at different points in the same solution for a given concentration. Also we measured the SERS spectra after preparing the three samples under the same condition of the rhodamine, Au, and Hg concentration.

Figure 1 illustrates our strategy of SERS detection of Hg(II) using SERS and fluorescence measurements of rhodamine dyes. As the mercury ion concentration increases, the amount of rhodamine dyes on Au NP surfaces should decrease on the other hand due to the preferential binding of rhodamine dyes

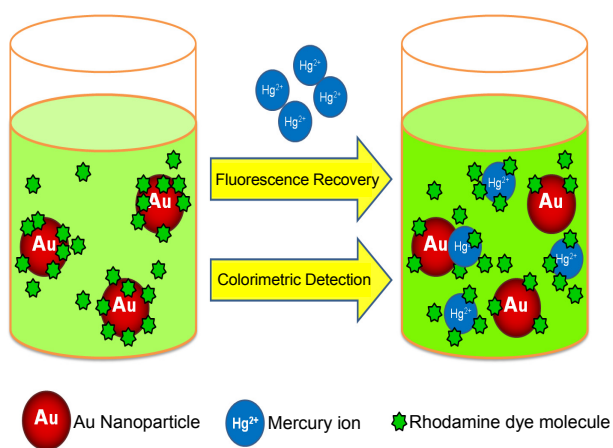


Figure 1. Our experimental scheme of Hg(II) using fluorescence quenching of rhodamine dyes on Au NPs.

Table 1. Absorption and emission band positions of Rh6G and Rh123^{a,b}

	Absorption Maximum	Emission Maximum
Rh6G	525	553
Rh123	500	525

^aUnit in nm. ^bConsistent with the data in refs. 19-23.

with the Hg ion. It is also possible that the mercury actually binds to the gold displacing the rhodamine dye. The fluorescence signal should be recovered as the Hg ion increases. Regarding the Raman intensity, as the fluorescence signal increases because of either the binding of rhodamine dyes and the Hg ions or the displacements reaction of rhodamine dyes by Hg,^{9,16} the SERS signal should decrease on the contrary. We can quantify the Hg(II) ion concentration in an aqueous solution by measuring the SERS intensities of rhodamine dyes on Au NPs. The calibration curves were obtained for the different batches to check the reproducibility.

Results and Discussion

Figure 2(a) shows a photo and absorption spectrum of Au nanoparticles. The maximum absorption is at ~520 nm. Figure 2(b) shows a representative transmission electron microscopic (TEM) image of particles.

Fluorescence Data. Figure 3 compares photos of fluorescent images of Rh6G and Rh123 before and after adding Au NPs and a small amount of Hg ions in the concentration range between 0 - 2.0 ppm. The fluorescence maxima of Rh6G and Rh123 were found at 553 and 525 nm, respectively, exhibiting their

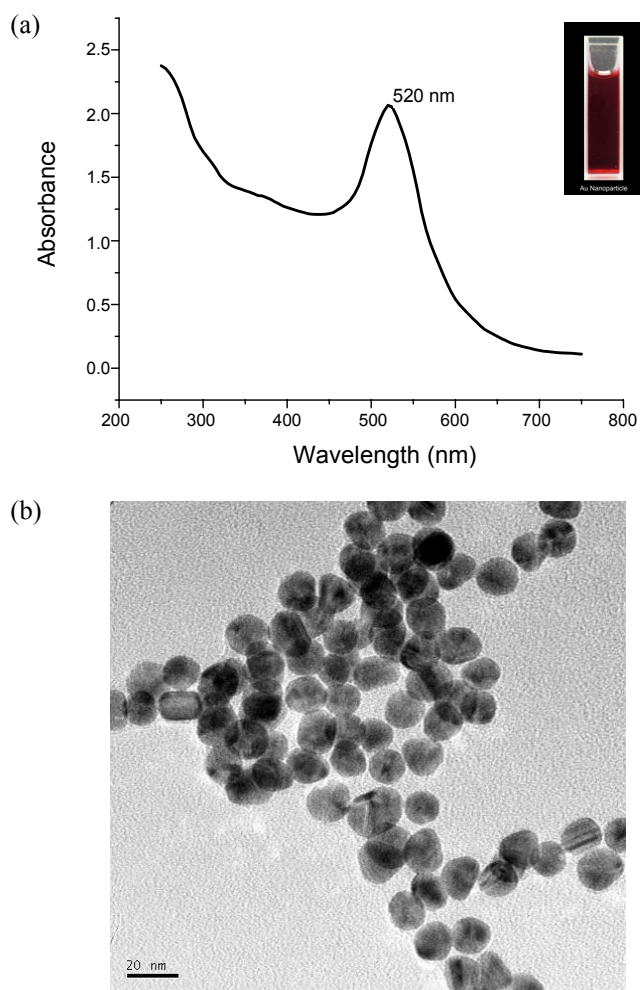


Figure 2. (a) Photo and absorption spectrum of Au NPs and (b) representative transmission electron microscopy (TEM) image of Au NPs.

own different colors. Although we found that the absorbance and emission maxima were slightly shifted by the concentrations of dyes,¹⁹ their positions in maxima were observed to be consistent with the previous reports.²⁰⁻²²

The fluorescent emission maximum of Rh123 appears to locate at somewhat closer to the absorption band of Au NPs. In the presence of Au NPs, the fluorescent intensities appeared to decrease because of the quenching effect as shown in Figure 3. Such a weakened fluorescent intensity was found to be recovered by adding the Hg ion in the concentration range between 0 ~ 2.0 ppm. When we added the Hg ions to rhodamine solutions containing the Au NPs, the reduced fluorescent intensities were found to be recovered as in the previous reports.^{15,16} We could observe the presence of the Hg ion in the concentration range of a few ppm from the color change. It is admitted that the absorption spectra of Au NPs can decrease the fluorescence intensities due to inner filter effects.¹⁸ Although we attempted to reduce this effect by decreasing the concentrations of Au NPs, it is expected that the emission maximum of Rh123 at ~525 nm could be more affected than that Rh6G at ~553 nm from the surface plasmon band of Au NPs at ~520 nm. This may explain why the photo images of Rh6G look better than those of Rh123. Figure 4 shows fluorescence recovery spectra of Rh6G in Au NP solution, when Hg(II) are added. To further investigate rho-

damine dyes' adsorption characteristics in detail, we performed SERS on the two rhodamine dyes on Au NPs.

SERS Spectra of Rh6G on Au NPs Depending on Hg Concentrations. Figure 5(a) shows Hg(II) concentration-dependent SERS spectra of Rh6G ($\sim 5 \times 10^{-6}$ M) in aqueous Au NPs in the range of 0.01 ~ 2.0 ppm. We could not find any direct evidence of the aggregation of Au NPs caused by the Hg(II) ion. Also as seen in the decrease of the SERS intensities by increase of the Hg ion concentration, a hot spot due to the aggregated particles for much larger SERS enhancements were not likely created for the Au structures under our experimental conditions. The

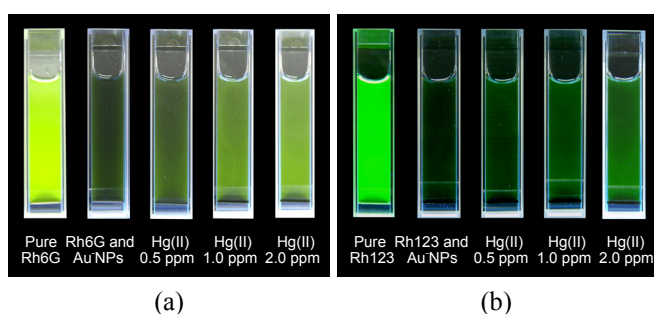


Figure 3. Fluorescence tests in the presence of Au NPs (~75 ppm) and Hg(II) (0 ~ 2.0 ppm). Photos of (a) Rh6G and (b) Rh123.

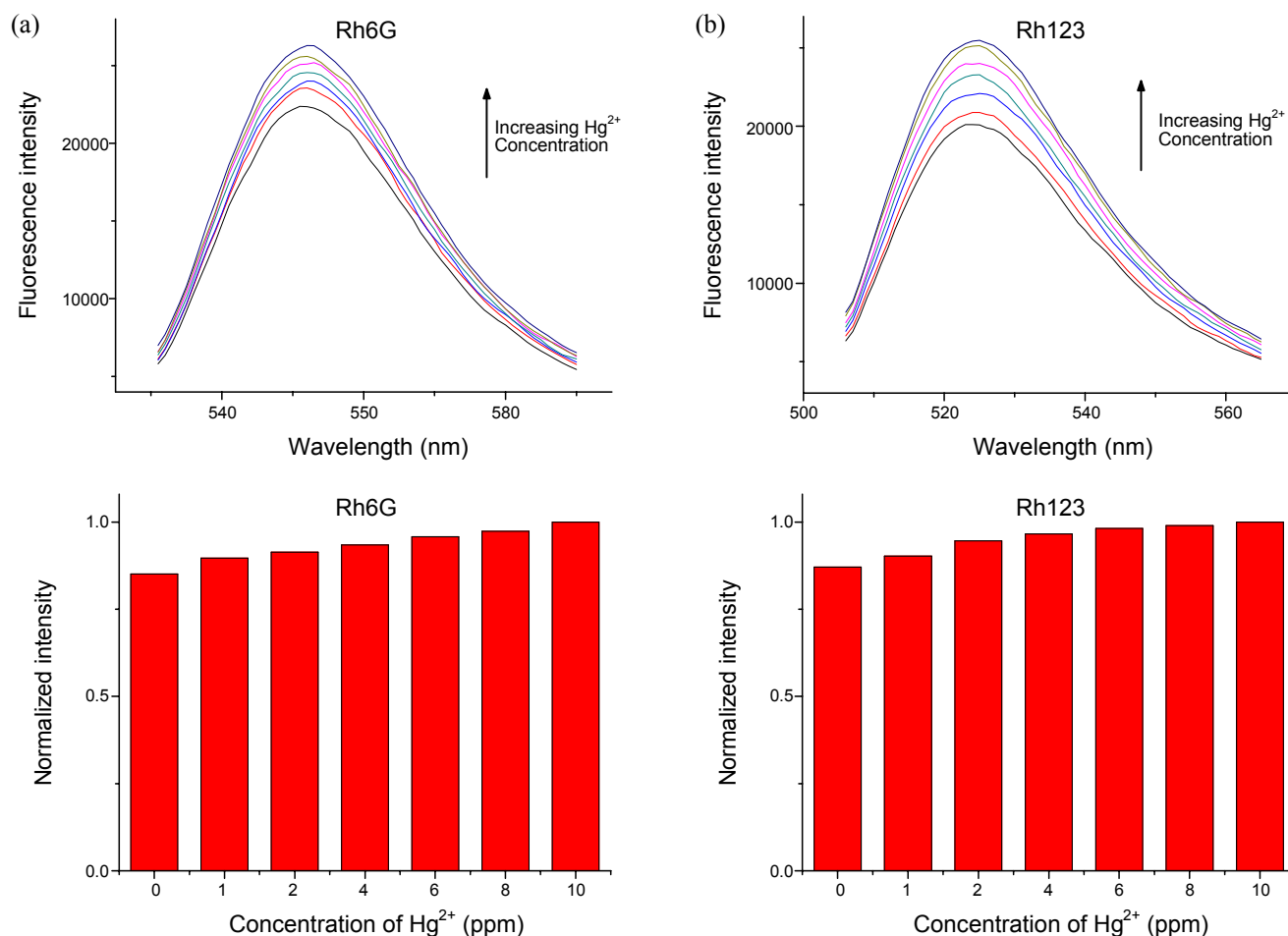


Figure 4. Fluorescence recovery spectra and their normalized intensities of (a) Rh6G and (b) Rh123 in Au NP solution, when Hg(II) are added.

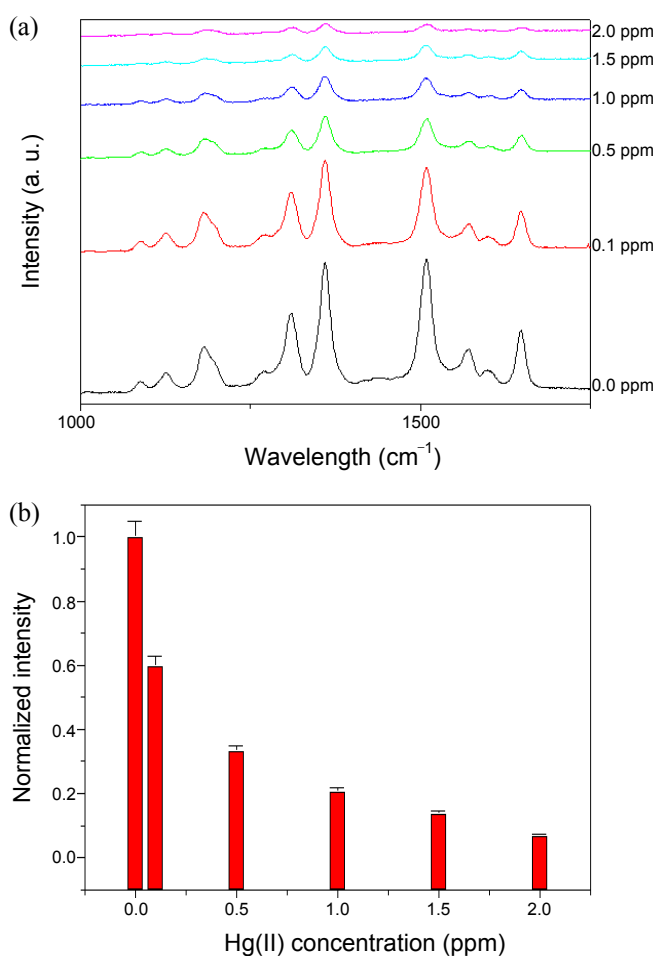


Figure 5. (a) Hg concentration-dependent SERS spectra of Rh6G ($\sim 5 \times 10^{-6}$ M) in aqueous Au NPs in the range of 0.01 ~ 2.00 ppm in the wavenumber region of 1000 - 1750 cm^{-1} . (b) Calibration curve for the Hg(II) concentration versus SERS intensity of Rh6G on Au NPs. The vibrational band at ~ 1359 cm^{-1} was used to compare the relative intensity. The error bars in the calibration curves indicate the standard deviations of the three measurements for differently-prepared samples.

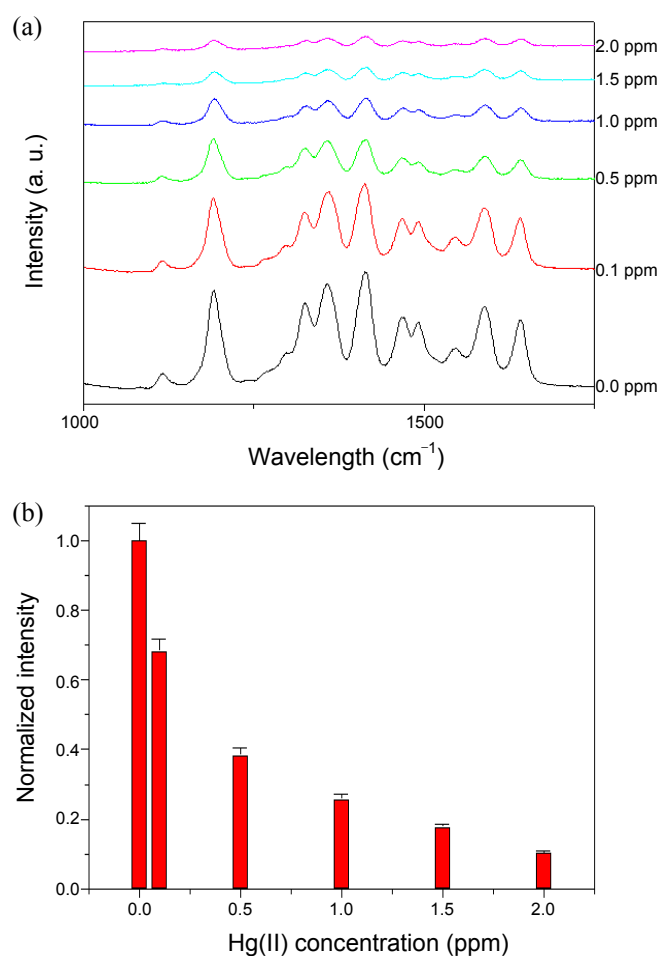


Figure 6. (a) Hg concentration-dependent SERS spectra of Rh123 ($\sim 5 \times 10^{-6}$ M) in aqueous Au NPs in the range of 0.01 ~ 2.00 ppm in the wavenumber region of 1000 - 1750 cm^{-1} . (b) Calibration curve for the Hg(II) concentration versus SERS intensity of Rh123 on Au NPs. The vibrational band at ~ 1191 cm^{-1} was used to compare the relative intensity. The error bars in the calibration curves indicate the standard deviations of the three measurements for differently-prepared samples.

prominent features between 1050 and 1650 cm^{-1} were assumed to be due to either xanthene or phenyl ring stretching modes.²³⁻²⁵

As the concentration of the Hg(II) increased, the SERS intensities decreased. Using this phenomena, we determined the Hg(II) concentration in an aqueous solution. Figure 5(b) shows the calibration curve for the Hg(II) concentration versus SERS intensity of Rh6G on Au NPs. One of the strongest vibrational band at ~ 1359 cm^{-1} in the SERS spectra of Rh6G was used to compare the relative intensity. We found that the decrease in SERS intensities could be reasonably well correlated with the increase of the Hg(II) concentration in the aqueous solution under our experimental condition. When the Hg(II) ion was added into the solution, the rhodamine dyes molecules appeared to detach from the Au NP surfaces as Figure 1 show.

SERS Spectra of Rh123 on Au NPs Depending on Hg Concentrations. Figure 6(a) and (b) illustrate the Hg concentration-dependent SERS spectra of Rh123 ($\sim 5 \times 10^{-6}$ M) in aqueous Au nanocolloids in the range of 0.01~2 ppm and the calibration curve for the Hg(II) concentration versus SERS intensity of

Rh123 on Au NPs, respectively. The prominent features between 1300 and 1650 cm^{-1} were assumed to be also due to either xanthene or phenyl ring stretching modes. One of the strongest vibrational band at ~ 1191 cm^{-1} for Rh123 was used to compare the relative intensity. This band was ascribed to the C-H bending of the xanthene ring in Rh123.¹³ We found that the adsorption behaviors of Rh6G and Rh123 inferred from the SERS study appeared to be analogous to each other in the Hg concentration region under our experimental condition.

The SERS spectral intensity did not show a linear relationship particular at a low concentration of Hg²⁺ under our experimental conditions. It is expected that more attenuation in signal intensities for the SERS spectra than the fluorescence data, since SERS should be more affected by the distance at the proximate region on the Au NP surfaces. This may be due to rather shorter distance dependence of SERS (d^{12}) than that of metal-induced fluorescence quenching (d^4).¹² If the adsorbate is not close to Au surfaces, the SERS signal is expected to be much weaker, exhibiting rather nonlinear behaviors. It has to be mentioned that

the SERS intensities should also be attributed to the coupling plasmon with neighboring Au NPs in an aggregate. These may make rather non-linear behaviors in our SERS measurements.

In this work, the fluorescence detection is one of the key factors to detect the Hg(II) ion in an aqueous solution. The surface-enhanced Raman scattering (SERS) tool was used to provide the supporting evidence on the adsorption mechanism on Au NP surfaces by providing the vibrational structures of rhodamine dyes. These two combined data of the fluorescence assays and vibrational analysis of the two different rhodamine dyes have not been performed in the previous reports.^{15,16} Technically, our experimental methods are substantially different from those using a microchip and a small volume of droplets.¹⁵ We have to mention that our data are not contradictory to those in the previous report, since rather higher concentrations of the Hg ions have been examined in the present work. The dynamic range of 0.1 ~ 20 ppb spanned far below our experimental Hg concentration of 100 ppb ~ 2000 ppb (0.1 ppm ~ 2 ppm). It is expected that SERS can be applied for more minute change in adsorption by optimizing the experimental conditions than the fluorescence discrimination. The advantage of our scheme lies in the easiness of gold nanoparticle-based colorimetry assay of the Hg (II) ion at a subppm concentration without much using complicated instruments.

The quenching effect from Au NPs is found to decrease as the Hg(II) concentration increased presumably due to the two possible processes of either the binding between rhodamine dyes and Hg ions or the Hg binding to the gold displacing the adsorbed rhodamine dye.^{9,16} To better provide a deeper insight of the Hg(II) detection mechanism of the rhodamine dyes on gold nanoparticle surfaces, we have employed the SERS technique combined with the vibrational analysis. Because their similar molecular structures of Rh6G and Rh123, their adsorption behaviors of Au NPs and detachment from the Hg surfaces appeared to be analogous. These dyes contain the nitrogen groups that can bind to either Au or Hg²⁺. To test the selectivity of our technique, we have worked on other ionic species beyond the Hg ion. Our preliminary results indicate other ionic species should show no similar result. In an aqueous solution, the adsorption and desorption of rhodamine dyes may occur with other possible mechanisms instead of binding to the Hg²⁺ ion, which makes a quantitative analysis rather problematic. Our experimental data however indicated that most desorption of the rhodamine dyes should be caused by binding to the Hg²⁺ ion, and thus be correlated with the concentrations of Hg²⁺ in a controlled manner under our experimental conditions. Our study should be helpful to design a fast and easy fluorescence Hg(II) sensor using citrate-reduced Au NPs and rhodamine dyes by understanding their adsorption characteristics.

Conclusions

We studied the adsorption of the two different rhodamine

dyes on Au NPs by changing the Hg(II) concentration in an aqueous solution. By monitoring the color change of rhodamine dyes, we detected an Hg(II) concentration as low as ~few ppm in an aqueous solution. Vibrational analysis was performed to study the rhodamine dye-Au NPs interactions to support our experimental observation. The advantage of our scheme lies in the easiness of gold nanoparticle-based assay of the Hg (II) ion at a concentration of a few ppm without much using complicated instruments.

Acknowledgments. This research was supported by the Basic Science Research Program through the National Research Foundation of Korea (NRF) funded by the Ministry of Education, Science, and Technology (2010-0001951).

References

1. Zahir, F.; Rizwi, S. J.; Haq, S. K.; Khan, R. H. *Environ. Toxicol. Pharmacol.* **2005**, *20*, 351.
2. Zheng, W.; Aschner, M.; Gherzi-Egea, J-F. *Toxicol. Appl. Pharmacol.* **2003**, *192*, 1.
3. Lewis, M.; Chancy, C. *Chemosphere* **2008**, *70*, 2016.
4. Vil'pan, Y. A.; Grinshtein, I. L.; Akatove, A. A.; Gucer, S. *Anal. Chem.* **2005**, *60*, 45.
5. Gao, T.; Lee, K. M.; Heo, J.; Yang, S. I. *Bull. Korean Chem. Soc.* **2010**, *31*, 2100.
6. Malashikhin, S. A.; Baldrige, K. K.; Finney, N. S. *Org. Lett.* **2010**, *5*, 940.
7. Han, N. S.; Shim, H. S.; Park, S. M.; Song, J. K. *Bull. Korean Chem. Soc.* **2009**, *30*, 2199.
8. Daniel, M-C.; Astruc, D. *Chem. Rev.* **2004**, *104*, 293.
9. Huang, C-C.; Chang, H-T. *Anal. Chem.* **2006**, *78*, 8332.
10. Lombardi, J. R.; Birke, R. L. *Acc. Chem. Res.* **2009**, *42*, 734.
11. Joo, S-W. *Bull. Korean Chem. Soc.* **2008**, *29*, 1761.
12. Schatz, G. C.; Van Duyne, R. P. In *Handbook of Vibrational Spectroscopy*; Chalmers, J. M., Griffiths, P. R., Eds.; John Wiley & Sons: New York, 2002; Vol.1, p 759.
13. Sarkar, J.; Chowdhury, J.; Pal, P.; Talapatra, G. B. *Vib. Spectrosc.* **2006**, *41*, 90.
14. Zamarion, V. M.; Timm, R. A.; Araki, K.; Toma, H. E. *Inorg. Chem.* **2008**, *47*, 2934.
15. Wang, G.; Lim, C.; Chen, L.; Chon, H.; Choo, J.; Hong, J.; deMello, A. J. *Anal. Bioanal. Chem.* **2009**, *394*, 1827.
16. Chen, J.; Zheng, A.; Chen, A.; Gao, Y.; He, C.; Kai, X.; Wu, G.; Chen, Y. *Anal. Chim. Acta* **2007**, *599*, 134.
17. Lee, P. C.; Meisel, D. *J. Phys. Chem.* **1982**, *86*, 3391.
18. Lakowicz, J. R. *Principles of Fluorescence Spectroscopy*, 3rd ed.; Springer: New York, USA., 2006; p 55.
19. Zhu, J.; Li, J-J.; Zhao, J-W. *Sens. Act. B* **2009**, *138*, 9-13.
20. Liu, B.; Liu, Z.; Cao, Z. *J. Luminesc.* **2006**, *118*, 99-105.
21. Griffiths, J.; Lee, W. J. *Dyes. Pigm.* **2003**, *57*, 107-114.
22. Emaus, R. K.; Grunwald, R.; Lemasters, J. J. *Biochim. Biophys. Acta* **1986**, *850*, 436.
23. Jensen, L.; Schatz, G. C. *J. Phys. Chem. A* **2006**, *110*, 5973.
24. Saini, G. S. S.; Amit, S.; Sarvpreet, K.; Bindra, K. S.; Vasant, S.; Tripathi, S. K.; Mhahajan, C. G. *J. Mol. Struct.* **2009**, *931*, 10.
25. Guthmuller, J.; Champagne, B. *ChemPhysChem.* **2008**, *9*, 1667.